# Constraints on the Higgs boson anomalous FCNC interactions with light quarks

M. Ilyushin[a], P. Mandrik[a,b], S. Slabospitsky[a]

[a]*NRC "Kurchatov Institute" - IHEP, Protvino, Moscow Region, Russia*
[b]*Moscow Institute of Physics and Technology, Dolgoprudny, Moscow Region, Russia*

## Abstract

We consider the Higgs boson anomalous FCNC interactions with $u$, $c$, $d$, $s$ and $b$ quarks using the effective field theory framework. Constraints on anomalous couplings are derived from experimental results on Higgs boson production with subsequent decay into $b\bar{b}$ pair at LHC with $\sqrt{s} = 13$ TeV. Upper limits on the branching fractions of $H \to b\bar{s}$ and $H \to b\bar{d}$ are set by performing a realistic detector simulation and accurately reproducing analysis selections of the CMS Higgs boson measurement in the four-lepton final state at $\sqrt{s} = 13$ TeV. The searches are projected into operation conditions of HL-LHC. Sensitivity at FCC-hh to anomalous FCNC interactions is studied based on Higgs boson production with $H \to \gamma\gamma$ decay channel. It is shown that at FCC-hh machine one can expect to set the upper limits of the order of $10^{-2}$ at 95% CL for $\mathcal{B}(H \to b\bar{s})$ and $\mathcal{B}(H \to b\bar{d})$.

*Keywords:* FCNC, Higgs, Flavor violation, LHC, HL-LHC, FCC-hh, EFT, Anomalous interactions, BSM, HEP

## 1. Introduction

The discovery of Higgs boson by the Large Hadron Collider (LHC) [1, 2] experiments has opened up new area of direct searches for physics Beyond Standard Model (BSM). One of the possible anomalous interaction is the Higgs-mediated flavour-changing neutral currents (FCNC). These processes are forbidden in Standard Model (SM) at tree level and are strongly suppressed in loop corrections by the Glashow-Iliopoulos-Maiani mechanism [3].

The Higgs mediated FCNC in top-quark sector is actively investigated at LHC [4–8] by searching for $t\bar{t}$ production with one top quark decay through

a FCNC channel and other follow the dominant SM decay $t \to bW$. The results of the searches are summarized in Table 1.

Table 1: The current experimental upper limits on FCNC decays of top-quark at 95% CL.

| Detector | $\mathcal{B}(t \to uH)$ | $\mathcal{B}(t \to cH)$ | Ref. |
|---|---|---|---|
| ATLAS, 13 TeV, 36.1 fb$^{-1}$ | $1.9 \times 10^{-3}$ | $1.6 \times 10^{-3}$ | [6] |
| CMS, 13 TeV, 35.9 fb$^{-1}$ | $4.7 \times 10^{-3}$ | $4.7 \times 10^{-3}$ | [8] |

The FCNC couplings of the Higgs to the rest SM quarks can affect various low-energy precision measurements. The strongest indirect bounds on FCNC quark-quark-Higgs couplings came from measurement of $B_{d,s} - \bar{B}_{d,s}$, $K^0 - \bar{K}^0$ and $D^0 - \bar{D}^0$ oscillations [9]. The corresponding constraints on FCNC couplings translated into upper limits on branching fractions of the FCNC decays of Higgs boson to $u, d, s, c, b$ quarks are summarized in the Table 2. Due to huge QCD background the experiments at LHC are less sensitive to searching for FCNC decays of the Higgs boson. On the other hand the direct probes of such processes could complement the indirect limits. In addition in possible BSM scenarios the branching ratio of $H \to qq'$ can be enhanced with keeping other low-energy flavour observables approximately at their SM values [10, 11]. Therefor, the searches for FCNC Higgs boson interactions are very important and could be considered as a complementary probe of new physics.

At the moment there is no any experimental evidence of the FCNC process. Future research and increase of the experimental sensitivity are related to the proposed energy-frontier colliders [12–15] such as High Luminosity LHC (HL-LHC) [16] and Future Circular Collider (FCC-hh) project, defined by the target of 100 TeV proton-proton collisions with a total integrated luminosity of 30 ab$^{-1}$ [17, 18].

In this article we invested the contribution of FCNC interactions to the single Higgs boson production (fig. 1, left) and Higgs boson production in association with a light quark (fig. 1, center and right). The limits on Higgs boson FCNC interactions based on recent LHC data are obtained and the searches are projected into operation conditions of HL-LHC [16] and FCC-hh projects. The cross section ratio for the different processes are presented in table 1.

Table 2: The upper limits on FCNC decays of Higgs boson to the light quarks at 95% CL from experiments with mesons (see [9] for details).

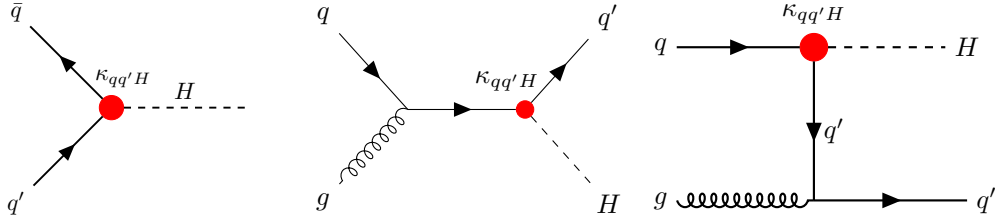| Observable | Constraint |
|---|---|
| $D^0$ oscillations | $\mathcal{B}(H \to u\bar{c}) \lesssim 2 \times 10^{-5}$ |
| $B_d^0$ oscillations | $\mathcal{B}(H \to d\bar{b}) \lesssim 8 \times 10^{-5}$ |
| $K^0$ oscillations | $\mathcal{B}(H \to d\bar{s}) \lesssim 2 \times 10^{-6}$ |
| $B_s^0$ oscillations | $\mathcal{B}(H \to s\bar{b}) \lesssim 7 \times 10^{-3}$ |



Figure 1: Example of diagrams for Higgs boson production (left) and Higgs boson associated production with quark (center and right) mediated by FCNC couplings.

3

## 2. The constraints from the current Higgs production cross-sections

The flavor-violating couplings may arise from different sources [19]. In this article we use the effective field theory approach (EFT) [20–22] for describing the effects of BSM physics in Higgs interactions. The effective Lagrangian (up to dimension-six gauge-invariant effective operators) has the form as follows [23, 24]:

$$\mathcal{L}_{BSM} = -\frac{1}{\sqrt{2}}\bar{q}(\kappa^L_{qq'H}P_L + \kappa^R_{qq'H}P_R)q'H \tag{1}$$

where $P_{L,R} = \frac{1}{2}(1\pm\gamma^5)$, $q, q' \in (u, c, t)$ or $q, q' \in (d, s, b)$. The couplings $\kappa^L_{qq'H}$ and $\kappa^R_{qq'H}$ are complex in general.

Note, that in our analysis these couplings are appeared in the combination

$$|\kappa^L_{qq'}|^2 + |\kappa^R_{qq'}|^2 = (\mathrm{Re}\,\kappa^L_{qq'})^2 + (\mathrm{Im}\,\kappa^L_{qq'})^2 + (\mathrm{Re}\,\kappa^R_{qq'})^2 + (\mathrm{Im}\,\kappa^R_{qq'})^2$$

Thus, in what follows we set

$$\left.\begin{array}{l} \kappa \equiv |\kappa^L_{qq'}| = |\kappa^R_{qq'}| \\ \lambda \equiv |\mathrm{Re}\,\kappa^L_{qq'}| = |\mathrm{Im}\,\kappa^L_{qq'}| = |\mathrm{Re}\,\kappa^R_{qq'}| = |\mathrm{Im}\,\kappa^R_{qq'}| \\ \rightarrow \kappa = \sqrt{2}\lambda \end{array}\right\} \tag{2}$$

The Higgs decays width resulted from (1) equals:

$$\Gamma(H \to q\bar{q}') = \frac{3(|\kappa^L_{qq'}|^2 + |\kappa^R_{qq'}|^2)M_H}{32\pi} = \frac{3|\kappa|^2 M_H}{16\pi} = |\lambda|^2 \times 14.92 \ \mathrm{GeV} \tag{3}$$

The very rough estimates of the coupling $\kappa_{qq'}$ could be obtained from the Higgs production in the $pp$-collisions at LHC [25, 26]:

$$pp \to H\,X, \ \ pp \to H\,W/ZX, \ \ H \to b\bar{b} \tag{4}$$

We use the experimental results from ATLAS and CMS collaborations:

$$\mu_b = \frac{\sigma^{exp}(pp \to H\,X)}{\sigma^{theor}(pp \to H\,X)} \tag{5}$$

| | $pp \to H\,W/Z\,X$ | $pp \to H\,X$ | |
|---|---|---|---|
| ATLAS | $\mu_b = 0.98^{+0.22}_{-0.21}$ | $\mu_b = 1.01 \pm 0.20$ | [25] |
| CMS | $\mu_b = 1.01 \pm 0.22$ | $\mu_b = 1.04 \pm 0.20$ | [26] |

and for estimates we set

$$0.8 \le \mu_b \le 1.2 \tag{6}$$

In order to get the constraints on anomalous constants $\kappa_{qq'}$ we consider the ratio:

$$\tilde{\mu}_b = \frac{\sigma(pp \to H)_{SM+FCNC} \, \mathcal{B}_{det}(H \to b\bar{b})_{SM+FCNC}}{\sigma(pp \to H)_{SM} \, \mathcal{B}_{det}(H \to b\bar{b})_{SM}} \tag{7}$$

where $(...)_{SM}$ and $(...)_{SM+FCNC}$ stands for SM and SM+FCNC contributions to Higgs production and decays. The value $\mathcal{B}_{det}$ equals branching fractions of the Higgs decays into quark-antiquark pair times the $B$-tagging and $B$ miss-tagging efficiencies (from ATLAS paper [25])

$$\varepsilon_b = 70\%, \ \varepsilon_c = 12\%, \ \varepsilon_q = 0.3\%, \ q = d, u, s \tag{8}$$

So, for SM and SM+FCNC scenarios we have:

$$\mathcal{B}_{det}(H \to b\bar{b})_{SM} = \mathcal{B}_{sm}(H \to b\bar{b})\varepsilon_b^2$$
$$\mathcal{B}_{det}(H \to b\bar{b})_{SM+FCNC} = B_{fcnc}(H \to b\bar{b})\varepsilon_b^2 + B_{fcnc}(H \to q_1\bar{q}_2)\varepsilon_{q_1}\varepsilon_{q_2}$$

We use the MG5_aMC@NLO 2.5.2 [27] package (see section 3) for estimation of the Higgs anomalous production cross-sections at $\sqrt{s} = 13$ TeV:

$$\sigma_{sm} \approx 50 \, \text{pb} \qquad \sigma(b\bar{s} + \bar{b}s)_{fcnc} = |\lambda|^2 \times 18000 \ \text{pb}$$
$$\sigma(b\bar{d} + \bar{b}d)_{anom} = |\lambda|^2 \times 45600 \, \text{pb} \qquad \sigma(c\bar{u} + \bar{c}u)_{anom} = |\lambda|^2 \times 82000 \, \text{pb}$$

Then, from requirement on $\tilde{\mu}_b$ from (6) we get the constraints on the anomalous couplings $\kappa_{qq'}$. To avoid ambiguities due to different normalizations of the couplings in the Lagrangian, the branching ratios of the corresponding FCNC processes are also used for presentation of the results.

Certainly, these constraints are much worse as indirect constraints, given if the Table 2. However, these constraints are first ones resulted from direct searches of the Higgs FCNC interactions with the light quarks.

## 3. Event generation

The estimation based on (7) does not take into account the differences in kinematics of the SM and FCNC Higgs boson production processes. In

Table 3: The upper limits on the anomalous couplings, the Higgs boson decay widths (in MeV) and branching fractions.

| $qq'$ | $\kappa$ | $\lambda$ | $\Gamma(q\bar{q}')$ MeV | $\mathcal{B}(q\bar{q}')$ |
|-------|----------|-----------|-------------------------|--------------------------|
| $bs$  | $\leq 0.0085$ | 0.006  | 0.54 | 10% |
| $bd$  | $\leq 0.0089$ | 0.0063 | 0.60 | 11% |
| $cu$  | $\leq 0.0096$ | 0.0068 | 0.69 | 13% |

order to accurately incorporate detector effects and reconstruction efficiencies for the next sections we are performing Monte-Carlo (MC) simulation of related processes. We use the Lagrangian (1) for the signal simulation. The Lagrangian (1) is implemented in FeynRules [28] based on [29] and the model is interfaced with generators using the UFO module [30]. The events are generated using the MG5_aMC@NLO 2.5.2 [27] package, with subsequent showering and hadronization in PYTHIA 8.230 [31]. The NNPDF3.0 [32] PDF sets are used. The detector simulation has been performed with the fast simulation tool DELPHES 3.4.2 [33] using the corresponding detectors parameterization cards. No additional pileup interactions are added to the simulation. The cross-sections for Higgs boson productions associated with zero or one jet and mediated by FCNC couplings in proton-proton collisions for different centre-of-mass energy are given in the Table 4. Note, these values are evaluated for Higss production with 0 or 1 jet using the MLM matching scheme [34]. Therefore, they are greater then those used in previous section.

## 4. Constrain from Higgs boson measurement in the four-lepton final state at $\sqrt{s} = 13$ TeV

In this section, we obtain upper the limit on the $\mathcal{B}(H \to b\bar{s})$ and $\mathcal{B}(H \to b\bar{d})$ branching fractions using constraints on Higgs boson measurement in the four-lepton final state at $\sqrt{s} = 13$ TeV from CMS experiment at LHC [35] from the reaction as follows:

$$p\,p \to H X, \; \to H\,j\,X, \quad H \to ZZ, \; Z \to \ell^+, \ell^-, \; \ell = \mu, e \qquad (9)$$

In order to accurately incorporate the effects of the analyses efficiency different for the SM and FCNC Higgs boson production we reproduce the events selections from [35].

Table 4: The cross-sections of Higgs boson + 0, 1 jet productions mediated by FCNC couplings in proton-proton collisions for different centre-of-mass energies.

| subprocess | Cross section, pb | | | |
|:---:|:---:|:---:|:---:|:---:|
| | 13 TeV | 14 TeV | 27 TeV | 100 TeV |
| $ucH$ | $9.08 \times 10^4 \lambda_{ucH}^2$ | $9.85 \times 10^4 \lambda_{ucH}^2$ | $2.01 \times 10^5 \lambda_{ucH}^2$ | $7.3 \times 10^5 \lambda_{ucH}^2$ |
| $dsH$ | $8.25 \times 10^4 \lambda_{dsH}^2$ | $9.02 \times 10^4 \lambda_{dsH}^2$ | $1.91 \times 10^5 \lambda_{dsH}^2$ | $7.23 \times 10^5 \lambda_{dsH}^2$ |
| $dbH$ | $4.81 \times 10^4 \lambda_{dbH}^2$ | $5.32 \times 10^4 \lambda_{dbH}^2$ | $1.18 \times 10^5 \lambda_{dbH}^2$ | $4.77 \times 10^5 \lambda_{dbH}^2$ |
| $sbH$ | $2.32 \times 10^4 \lambda_{sbH}^2$ | $2.61 \times 10^4 \lambda_{sbH}^2$ | $6.67 \times 10^4 \lambda_{sbH}^2$ | $3.27 \times 10^5 \lambda_{sbH}^2$ |

The four-lepton candidates build $ZZ$ pairs. One $Z$ candidate is defined as pairs of two opposite charge and matching flavour leptons ($e^+e^-, \mu^+\mu^-$) that satisfy $12 < m_{ll} < 120$ GeV. Electrons are reconstructed within the geometrical acceptance defined by pseudorapidity $|\eta^e| < 2.5$ and for transverse momentum $p_T^e > 7$ GeV. Muons are reconstructed within the geometrical acceptance $|\eta^\mu| < 2.4$ and $p_T^\mu > 5$ GeV. All leptons within $ZZ$ pairs must be separated in angular space by at least $\Delta R(l_i, l_j) > 0.02$. Two of the four selected leptons should have $p_{T,i} > 20$ GeV and $p_{T,j} > 10$ GeV.

The $Z$ candidate with reconstructed mass $m_{ll}$ closest to the nominal $Z$ boson mass is denoted as $Z_1$, and the second one is denoted as $Z_2$. The $Z_1$ invariant mass must be larger than 40 GeV. In the $4\mu$ and $4e$ sub-channels the $ZZ$ event with reconstructed mass $m_{Z2} \geq 12$ GeV and $m_{Z1}$ closest to the nominal $Z$ boson mass. All four opposite-charge lepton pairs that can be built with the four leptons (irrespective of flavor) are required to satisfy $m_{l_i^+ l_j^-} > 4$ GeV. Finally, the four-lepton invariant mass should be of the Higgs boson in a $118 < m_{4l} < 130$ GeV.

The comparison of selection efficiencies for FCNC Higgs boson production processes are presented in Table 5. The simulation of the SM Higgs boson production with Delphes show good agreement with reference Geant4 results taken from [35]. The selection efficiency is different for different FCNC Higgs boson productions processes due to the presence of the valence $d$ quark in $bdH$ vertex (as compared to $bs \to H$ production).

Statistical analyses is performed based on the number of selected events (after the cut on $118 < m_{4l} < 130$ GeV) where the expected number of signal

Table 5: The comparison of selection efficiency for FCNC and SM Higgs boson productions for different $ZZ$ decay channels before the cut on invariant mass reconstructed Higgs boson $m_{4l} \in [118, 130]$ GeV and after the cut. The reference Geant4 results are taken from [35].

| Higgs production | $4e$ | $2e2\mu$ | $4\mu$ | total | total ($m_{4l}$ cut) |
|---|---|---|---|---|---|
| SM (Geant4) | 5.1% | 12.9% | 10.2% | 28.3% | 24.9% |
| SM (Delphes) | 4.9% | 13.1% | 9.3% | 27.2% | 25.6% |
| FCNC ($dbH$) | 3.6% | 9.5% | 6.5% | 19.5% | 17.8% |
| FCNC ($sbH$) | 4.9% | 12.8% | 9% | 26.7% | 24.5% |

FCNC events is from our modeling and the observed and expected number of background events are taken from the CMS experimental results [35]. For the signal processes lepton energy resolution (20%), lepton energy scale (0.3%), lepton identification (9% on the overall event yield) and luminosity (2.6%) uncertainties are taken into account. The uncertainty from the renormalization and factorization scale is determined by varying these scales between 0.5 and 2 times their nominal value while keeping their ratio between 0.5 and 2 [36]. PDF uncertainty is determined by taking the root mean square of the variation when using different replicas of the default PDF set [37]. Contributions of the systematic uncertainties to selection efficiency of the FCNC Higgs boson production are summarized in the Table 6. The total uncertainties on the number of selected signal and background (extracted from [35]) events are incorporated into statistical model as a nuisances neglecting the correlations.

Bayesian inference is used to derive the posterior probability based on the following likelihood function:

$$\mathcal{L} = \mathcal{G}\left(N_{obs}|N_{back} + (N_{SM} + N_{FCNC}) \cdot \frac{\mathcal{B}_{FCNC+SM}}{\mathcal{B}_{SM}}, \sqrt{N_{obs}}\right) \times$$
$$\times \mathcal{G}\left(N_{back}|N_{back}^{exp}, \sigma_{N_{back}^{exp}}\right) \times$$
$$\times \mathcal{G}\left(N_{FCNC}|N_{FCNC}^{exp}(\lambda), \sigma_{N_{FCNC}^{exp}(\lambda)}\right)$$

where the $\mathcal{G}$ - Gaussian function, $N_{back}^{exp}, N_{SM}^{exp}, N_{FCNC}^{exp}$ - the expected from the MC simulation number of background, SM and FCNC Higgs boson production events respectively, $\sigma_{N_{...}^{exp}}$ - its uncertainty, $\mathcal{B}_{FCNC+SM}$ - branching of

Table 6: Summary of contribution of the systematic uncertainties to the selection efficiency of the FCNC Higgs boson production.

| Process | $\mathcal{B}(H \to b\bar{s})$ | $\mathcal{B}(H \to b\bar{d})$ |
|---|---|---|
| Lepton energy resolution | $< \pm 0.2\%$ | $< \pm 0.2\%$ |
| Lepton energy scale | $< \pm 0.5\%$ | $< \pm 0.5\%$ |
| Lepton identification | $\pm 9\%$ | $\pm 9\%$ |
| Luminosity | $\pm 2.6\%$ | $\pm 2.6\%$ |
| QCD scale | $-19.6\% +18.1$ | $-17\% +15.2\%$ |
| PDF | $\pm 8\%$ | $\pm 3.4$ |
| Total | $-23.1\% +21.9\%$ | $-19.7\% +18.2\%$ |

$H \to 4\ell$ ($\ell = e, \mu$) in the presence of FCNC.

The 95% C.L. expected exclusion limits on the anomalous couplings and the branching fractions are given in Table 8.

## 5. Sensitivity at HL-LHC

The reconstruction efficiency estimated in section 4 can be used to project the FCNC searches into HL-LHC conditions, defined by total integrated luminosity of 3 ab$^{-1}$ and collision energy of 14 TeV, respectively. For the rescaling the crossections of SM Higgs boson productions are taken from [38]. The rescaling factors for crossections of $qq \to ZZ$ and $gg \to ZZ$ background processes are taken from [39]. The rescaling factros for crossections of "$Z + X$" background processes is estimated using the corresponding crossections from MG5_aMC@NLO 2.5.2 [27] simulation of dominated $Z + jets$ process. The cross section ratio for the different processes are summurised in table 7. Statistical analyses from section 4 is reproduced for the new conditions. The dominated systematic uncertainties on the simulation originating from theoretical sources are scaled by 50% following the treatment of systematic uncertainties in [38]. In this considered scenario the theoretical uncertainties are expected to improve over time due to developments in the calculations, techniques and orders considered. The 95% C.L. expected

9

exclusion limits on the anomalous couplings and the branching fractions are given in Table 8.

Table 7: Cross section ratios $\sigma_{14\ \mathrm{TeV}}/\sigma_{13\ \mathrm{TeV}}$ for FCNC and background processes.

| **Process** | $\sigma_{14\ \mathrm{TeV}}/\sigma_{13\ \mathrm{TeV}}$ |
| --- | --- |
| $qq \to ZZ$ | 1.17 |
| $gg \to ZZ$ | 1.13 |
| "$Z + X$" | 1.11 |
| SM Higgs | 1.13 |
| FCNC Higgs ($dbH$) | 1.10 |
| FCNC Higgs ($sbH$) | 1.13 |

## 6. Sensitivity at FCC-hh

In this section the sensitivity to single Higgs boson production through FCNC in $bdH$ and $bsH$ subprocesses is explored for the FCC-hh experimental conditions following the [40] SM study. The $H \to \gamma\gamma$ decay channel is used in this analysis. The SM single Higgs production is considered as background in additional to QCD di-photon productions including the huge tree level $qq \to \gamma\gamma$ component, generated up to two merged extra-jets, and a smaller loop-induced component, $gg \to \gamma\gamma$, generated up to one additional merged jet. A conservative K-factor of 2 is applied to both QCD contributions. The signal and background process generation and detector simulation are described in 3 chapter.

The photons with $p_T > 25$ GeV, $|\eta| < 4$ and relative isolation $< 0.15$ are used in the following analyses. Jets are reconstructed using anti$-kT$ algorithm with distance parameter $R = 0.4$ and required to have $p_T > 30$ GeV, $|\eta| < 3$. The events are selected using the following baseline criteria:

1. at least 2 selected photons and at least one of them with $p_T > 30$ GeV;
2. mass of the Higgs boson candidate reconstructed from the two photons with the highest $p_T$ should be $|m_H - 125| < 5$ GeV.
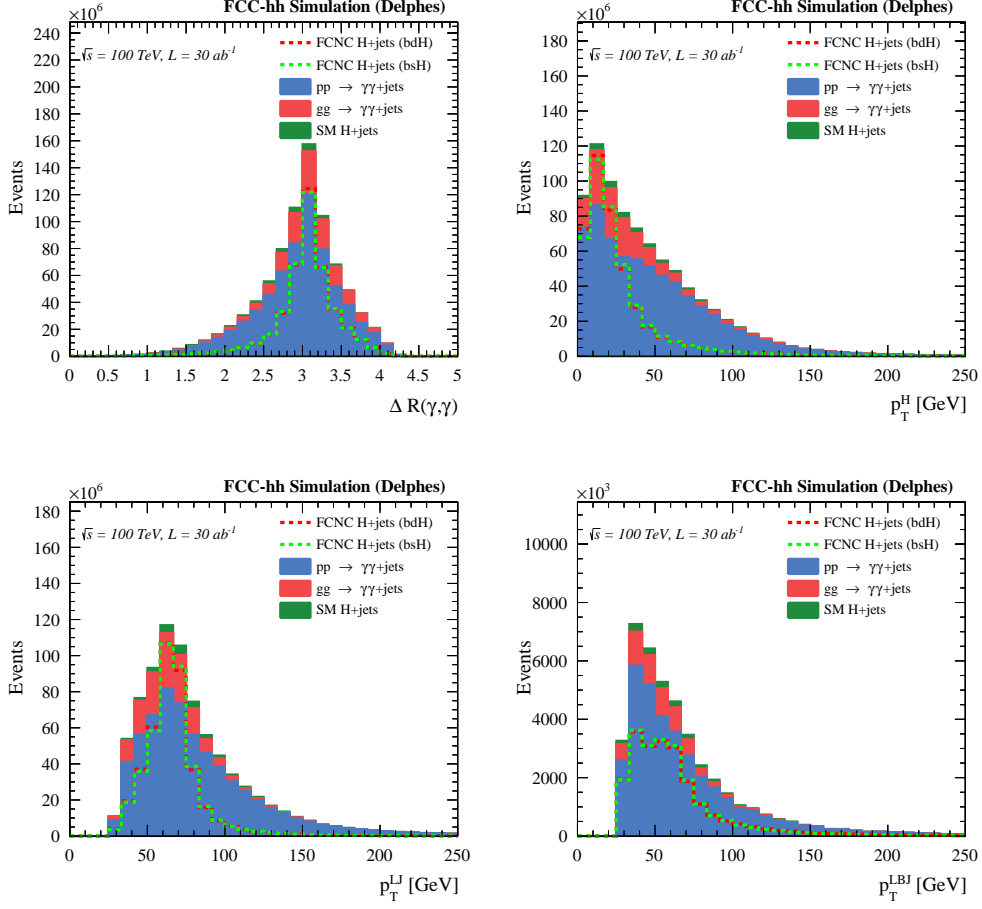
Figure 2: Distributions of the kinematic variables obtained after basic selections: $\Delta R$ between two selected photons with the highest $p_T$ (top-left), $p_T$ of the Higgs boson candidate (top-right), $p_T$ of the leading jet (bottom-left), $p_T$ of the leading b-tagged jet (bottom-right). The signal processes have arbitrary normalization for the illustration purpose.
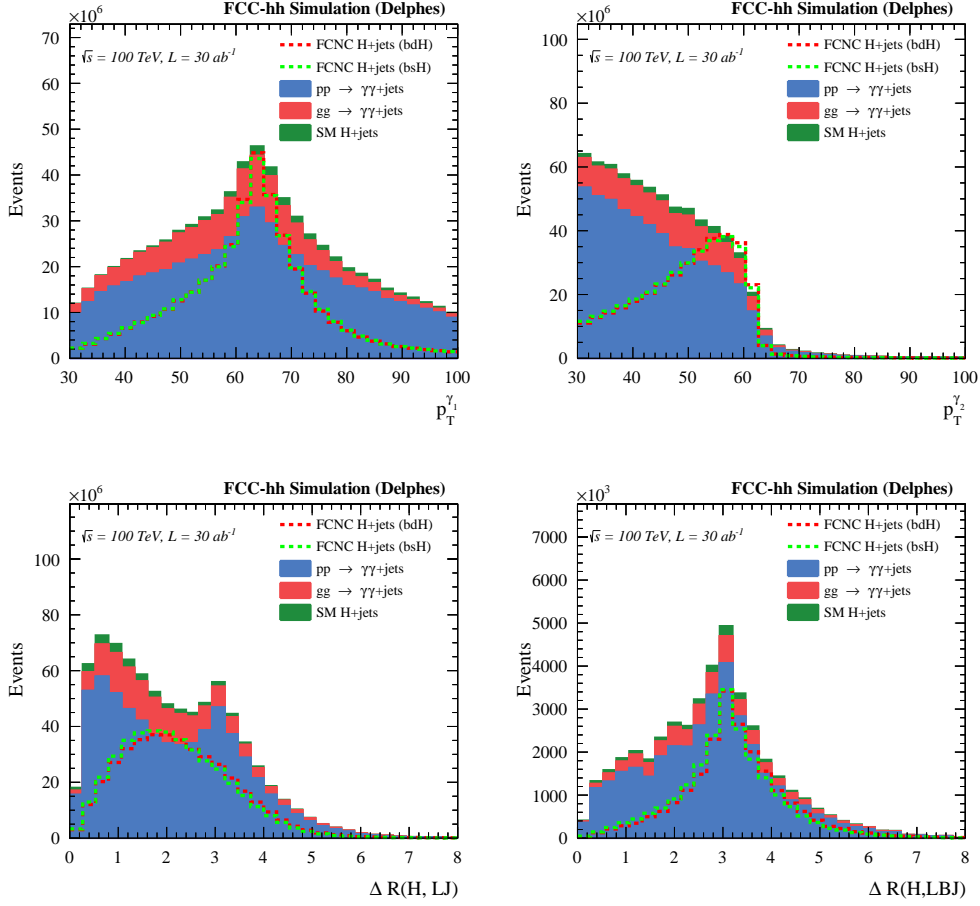
11

Figure 3: Distributions of the kinematic variables obtained after basic selections: leading photons $p_T^{\gamma_1}$ (top-left), second photons $p_T^{\gamma_2}$ (top-right), $\Delta R$ between Higgs boson candidate and leading jet (bottom-left), $\Delta R$ between Higgs boson candidate and leading b-tagged jet (bottom-right). The signal processes have arbitrary normalization for the illustration purpose.
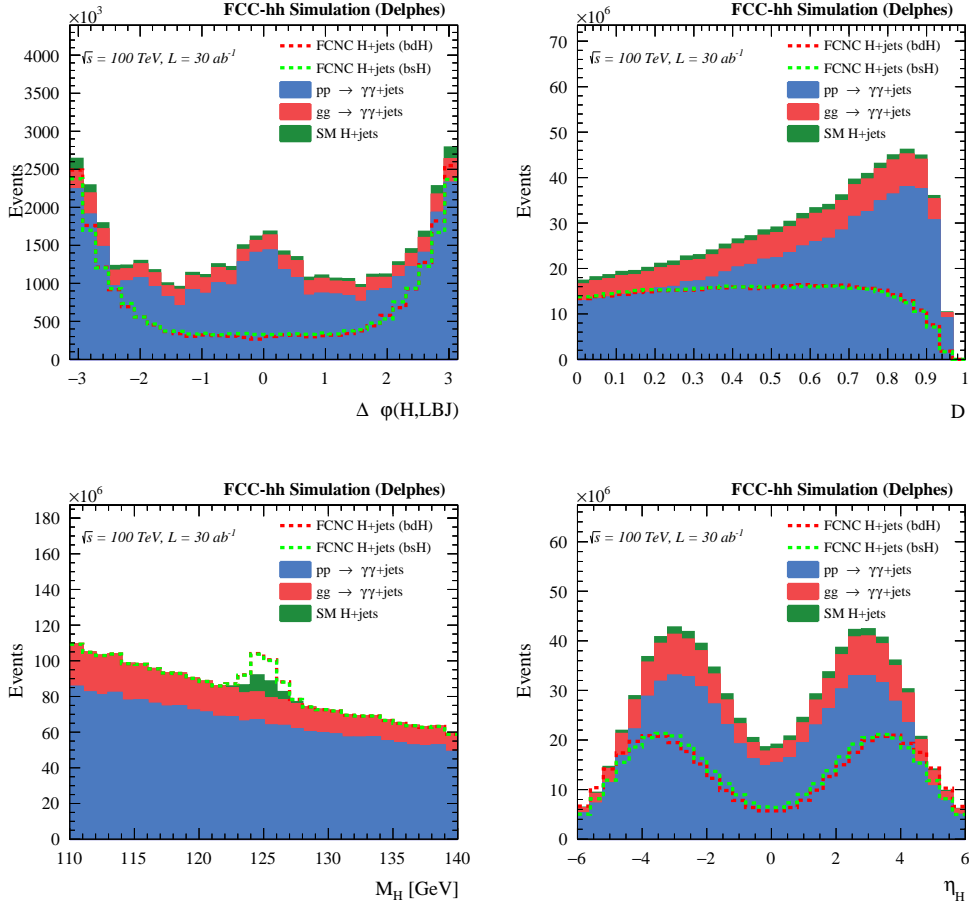
Figure 4: Distributions of the kinematic variables obtained after basic selections: $\Delta\varphi$ between reconstructed Higgs boson candidate and leading b-tagged jet (top-left), disbalance in energy of photons from Higgs decay (top-right, see text for the description) and mass of the reconstructed Higgs boson candidate (bottom-left, without cut on mass), $\eta$ of the reconstructed Higgs boson candidate (bottom-right). The signal processes have arbitrary normalization for the illustration purpose.
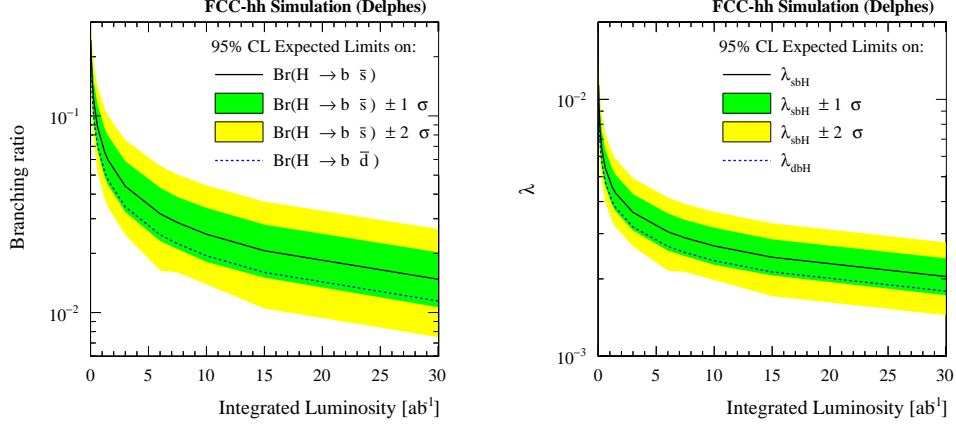
Figure 5: Expected exclusion limits at 95% C.L. on the FCNC $H \to b\bar{s}$ and $H \to b\bar{d}$ branching fractions (left) and FCNC couplings (right) as a function of integrated luminosity.

Distributions of the kinematic variables obtained after baseline selections are presented at Fig. 2, Fig. 3 and Fig. 4.

A Boosted Decision Tree (BDT) constructed in the TMVA framework [41] is used to separate the signal signature from the background contributions. 10% of events selected for training and the remainder are used in the statistical analysis of the BDT discriminants with the CombinedLimit package. The following input variables are used for training:

1. Higgs boson candidate $M_H$, $p_T^H$ and $\eta_H$;
2. leading jet (LJ) $p_T^{LJ}$ and $\eta_{LJ}$;
3. leading b-tagged jet (LBJ) $p_T^{LBJ}$ and $\eta_{LBJ}$;
4. leading photons $p_T^{\gamma_1}$, $\eta^{\gamma_1}$ and second photons $p_T^{\gamma_2}$, $\eta^{\gamma_2}$;
5. Number of jets $N_{jets}$ and number of b-tagged jets $N_{b-jets}$;
6. $\Delta R(\gamma, \gamma)$ between leading and second photon;
7. $\Delta R(H, LBJ)$ between Higgs boson candidate and leading jet;
8. $\Delta R(H, LJ)$ between Higgs boson candidate and leading b-tagged jet.

For each background a 20% normalisation uncertainty is assumed and incorporated in statistical model as nuisance parameter. The asymptotic frequentist formulae [42] is used to obtain an expected upper limit on signal cross section based on an Asimov data set of background-only model. The

14

Table 8: The 95% C.L. expected exclusion limits at FCC-hh on the branching fractions of Higgs FCNC decays and flavor-violating couplings in comparison with present experimental limits.

| Experiment | $\mathcal{B}(H \to b\bar{s})$ | $\mathcal{B}(H \to b\bar{d})$ |
|---|---|---|
| Meson oscillations [9] | $7 \times 10^{-3}$ | $8 \times 10^{-5}$ |
| CMS LHC $H \to ZZ \to 4\ell$ (35.9 fb$^{-1}$, 13 TeV) | $27 \times 10^{-2}$ | $32 \times 10^{-2}$ |
| HL-LHC $H \to ZZ \to 4\ell$ (3 ab$^{-1}$, 14 TeV) | $5.8 \times 10^{-2}$ | $6.0 \times 10^{-2}$ |
| FCC-hh $H \to \gamma\gamma$ (30 ab$^{-1}$, 100 TeV) | $1.5 \times 10^{-2}$ | $1.1 \times 10^{-2}$ |
| Experiment | $\lambda_{sbH}$ | $\lambda_{dbH}$ |
| Meson oscillations [9] | $1.9 \times 10^{-3}$ | $2.1 \times 10^{-4}$ |
| CMS LHC $H \to ZZ \to 4\ell$ (35.9 fb$^{-1}$, 13 TeV) | $13 \times 10^{-3}$ | $14 \times 10^{-3}$ |
| HL-LHC $H \to ZZ \to 4\ell$ (3 ab$^{-1}$, 14 TeV) | $4.0 \times 10^{-3}$ | $4.1 \times 10^{-3}$ |
| FCC-hh $H \to \gamma\gamma$ (30 ab$^{-1}$, 100 TeV) | $2.0 \times 10^{-3}$ | $1.8 \times 10^{-3}$ |

95% C.L. expected exclusion limits on the branching fractions are given in Table 8. Figure 5 shows the expected exclusion limits at 95% C.L. on the FCNC $H \to b\bar{s}$ and $H \to b\bar{d}$ branching fractions and FCNC couplings as a function of integrated luminosity.

## 7. Conclusions

In this work, we demonstrate that the contribution of flavour violation interaction to the production of the Higgs boson in high energy proton-proton collisions can be used for the direct search. The realistic detector simulation and accurately reproducing analysis selections of the CMS Higgs boson measurement in the four-lepton final state at $\sqrt{s} = 13$ TeV allow to set upper limits on the branching fractions of $H \to b\bar{s}$ and $H \to b\bar{d}$ and project the searches into HL-LHC conditions. We also examine the sensitivity at FCC-hh based on Higgs boson production with $H \to \gamma\gamma$ decay channel. Expected upper limits of the order of $10^{-2}$ at 95% CL for $\mathcal{B}(H \to b\bar{s})$ and $\mathcal{B}(H \to b\bar{d})$ are competitive with the indirect limits from meson oscillations experiments. The outcome of our study is summarised in Table 8. Further improvements

are possible through the combination of results of different Higgs boson decay and interaction searhes such as pair Higgs boson production.

## Acknowledgments

## References

[1] G. Aad, et al., Observation of a new particle in the search for the Standard Model Higgs boson with the ATLAS detector at the LHC, Phys. Lett. B716 (2012) 1–29. `arXiv:1207.7214`, `doi:10.1016/j.physletb.2012.08.020`.

[2] S. Chatrchyan, et al., Observation of a new boson at a mass of 125 GeV with the CMS experiment at the LHC, Phys. Lett. B716 (2012) 30–61. `arXiv:1207.7235`, `doi:10.1016/j.physletb.2012.08.021`.

[3] S. L. Glashow, J. Iliopoulos, L. Maiani, Weak interactions with lepton-hadron symmetry, Phys. Rev. D 2 (1970) 1285–1292. `doi:10.1103/PhysRevD.2.1285`.

[4] G. Aad, et al., Search for flavour-changing neutral current top quark decays $t \to Hq$ in $pp$ collisions at $\sqrt{s} = 8$ TeV with the ATLAS detector, JHEP 12 (2015) 061. `arXiv:1509.06047`, `doi:10.1007/JHEP12(2015)061`.

[5] M. Aaboud, et al., Search for top quark decays $t \to qH$, with $H \to \gamma\gamma$, in $\sqrt{s} = 13$ TeV $pp$ collisions using the ATLAS detector, JHEP 10 (2017) 129. `arXiv:1707.01404`, `doi:10.1007/JHEP10(2017)129`.

[6] M. Aaboud, et al., Search for flavor-changing neutral currents in top quark decays $t \to Hc$ and $t \to Hu$ in multilepton final states in proton–proton collisions at $\sqrt{s} = 13$ TeV with the ATLAS detector`arXiv:1805.03483`.

[7] V. Khachatryan, et al., Search for top quark decays via Higgs-boson-mediated flavor-changing neutral currents in pp collisions at $\sqrt{s}$ = 8 TeV, JHEP 02 (2017) 079. `arXiv:1610.04857, doi:10.1007/JHEP02(2017)079.`

[8] A. M. Sirunyan, et al., Search for the flavor-changing neutral current interactions of the top quark and the Higgs boson which decays into a pair of b quarks at $\sqrt{s}$ = 13 TeV`arXiv:1712.02399, doi:10.1007/JHEP06(2018)102.`

[9] R. Harnik, J. Kopp, J. Zupan, Flavor Violating Higgs Decays, JHEP 03 (2013) 026. `arXiv:1209.1397, doi:10.1007/JHEP03(2013)026.`

[10] A. Crivellin, J. Heeck, D. Mller, Large $h \to bs$ in generic two-Higgs-doublet models, Phys. Rev. D97 (3) (2018) 035008. `arXiv:1710.04663, doi:10.1103/PhysRevD.97.035008.`

[11] W. Altmannshofer, B. Maddock, D. Tuckler, Rare Top Decays as Probes of Flavorful Higgs Bosons`arXiv:1904.10956.`

[12] P. Mandrik, Top FCNC searches at HL-LHC with the CMS experiment, EPJ Web Conf. 191 (2018) 02009. `arXiv:1808.09915, doi:10.1051/epjconf/201819102009.`

[13] D. Barducci, A. J. Helmboldt, Quark flavour-violating Higgs decays at the ILC, JHEP 12 (2017) 105. `arXiv:1710.06657, doi:10.1007/JHEP12(2017)105.`

[14] P. Mandrik, Prospect for top quark FCNC searches at the FCC-hh, in: 4th International Conference on Particle Physics and Astrophysics (ICPPA 2018) Moscow, Russia, October 22-26, 2018, 2018. `arXiv:1812.00902.`

[15] M. A. Arroyo-Urea, R. Gaitn-Lozano, J. H. Montes de Oca Y., E. A. Herrera-Chacn, T. A. Valencia-Prez, Search for the $t \to ch$ decay at hadron colliders`arXiv:1903.02718.`

[16] G. Apollinari, I. Bjar Alonso, O. Brning, M. Lamont, L. Rossi, High-Luminosity Large Hadron Collider (HL-LHC): Preliminary Design Report, CERN Yellow Reports: Monographs, CERN, Geneva, 2015. URL `https://cds.cern.ch/record/2116337`

[17] M. Benedikt, et al., Future Circular Collider, Tech. Rep. CERN-ACC-2018-0058, CERN, Geneva, submitted for publication to Eur. Phys. J. ST. (Dec 2018).
URL http://cds.cern.ch/record/2651300

[18] M. Mangano, et al., Future Circular Collider, Tech. Rep. CERN-ACC-2018-0056, CERN, Geneva, submitted for publication to Eur. Phys. J. C. (Dec 2018).
URL http://cds.cern.ch/record/2651294

[19] K. Agashe, et al., Working Group Report: Top Quark, in: Proceedings, 2013 Community Summer Study on the Future of U.S. Particle Physics: Snowmass on the Mississippi (CSS2013): Minneapolis, MN, USA, July 29-August 6, 2013, 2013. arXiv:1311.2028.
URL https://inspirehep.net/record/1263763/files/arXiv:1311.2028.pdf

[20] S. Weinberg, Phenomenological Lagrangians, Physica A96 (1-2) (1979) 327–340. doi:10.1016/0378-4371(79)90223-1.

[21] W. Buchmuller, D. Wyler, Effective Lagrangian Analysis of New Interactions and Flavor Conservation, Nucl. Phys. B268 (1986) 621–653. doi:10.1016/0550-3213(86)90262-2.

[22] C. Arzt, M. B. Einhorn, J. Wudka, Patterns of deviation from the standard model, Nucl. Phys. B433 (1995) 41–66. arXiv:hep-ph/9405214, doi:10.1016/0550-3213(94)00336-D.

[23] J. A. Aguilar-Saavedra, Top flavor-changing neutral interactions: Theoretical expectations and experimental detection, Acta Phys. Polon. B35 (2004) 2695–2710. arXiv:hep-ph/0409342.

[24] J. A. Aguilar-Saavedra, A Minimal set of top-Higgs anomalous couplings, Nucl. Phys. B821 (2009) 215–227. arXiv:0904.2387, doi:10.1016/j.nuclphysb.2009.06.022.

[25] M. Aaboud, et al., Observation of $H \to b\bar{b}$ decays and $VH$ production with the ATLAS detector, Phys. Lett. B786 (2018) 59–86. arXiv:1808.08238, doi:10.1016/j.physletb.2018.09.013.

[26] A. M. Sirunyan, et al., Observation of Higgs boson decay to bottom quarks, Phys. Rev. Lett. 121 (12) (2018) 121801. `arXiv:1808.08242`, `doi:10.1103/PhysRevLett.121.121801`.

[27] J. Alwall, R. Frederix, S. Frixione, V. Hirschi, F. Maltoni, O. Mattelaer, H. S. Shao, T. Stelzer, P. Torrielli, M. Zaro, The automated computation of tree-level and next-to-leading order differential cross sections, and their matching to parton shower simulations, JHEP 07 (2014) 079. `arXiv:1405.0301`, `doi:10.1007/JHEP07(2014)079`.

[28] A. Alloul, N. D. Christensen, C. Degrande, C. Duhr, B. Fuks, FeynRules 2.0 - A complete toolbox for tree-level phenomenology, Comput. Phys. Commun. 185 (2014) 2250–2300. `arXiv:1310.1921`, `doi:10.1016/j.cpc.2014.04.012`.

[29] A. Amorim, J. Santiago, N. Castro, R. Santos, `http://feynrules.irmp.ucl.ac.be/wiki/GeneralFCNTop`.

[30] C. Degrande, C. Duhr, B. Fuks, D. Grellscheid, O. Mattelaer, T. Reiter, UFO - The Universal FeynRules Output, Comput. Phys. Commun. 183 (2012) 1201–1214. `arXiv:1108.2040`, `doi:10.1016/j.cpc.2012.01.022`.

[31] T. Sjstrand, S. Ask, J. R. Christiansen, R. Corke, N. Desai, P. Ilten, S. Mrenna, S. Prestel, C. O. Rasmussen, P. Z. Skands, An Introduction to PYTHIA 8.2, Comput. Phys. Commun. 191 (2015) 159–177. `arXiv:1410.3012`, `doi:10.1016/j.cpc.2015.01.024`.

[32] R. D. Ball, et al., Parton distributions for the LHC Run II, JHEP 04 (2015) 040. `arXiv:1410.8849`, `doi:10.1007/JHEP04(2015)040`.

[33] J. de Favereau, C. Delaere, P. Demin, A. Giammanco, V. Lemaître, A. Mertens, M. Selvaggi, Delphes 3: a modular framework for fast simulation of a generic collider experiment, Journal of High Energy Physics 2014 (2) (2014) 57. `doi:10.1007/JHEP02(2014)057`.
URL `https://doi.org/10.1007/JHEP02(2014)057`

[34] J. Alwall, et al., Comparative study of various algorithms for the merging of parton showers and matrix elements in hadronic collisions, Eur. Phys. J. C53 (2008) 473–500. `arXiv:0706.2569`, `doi:10.1140/epjc/s10052-007-0490-5`.

[35] A. M. Sirunyan, et al., Measurements of properties of the Higgs boson decaying into the four-lepton final state in pp collisions at $\sqrt{s} = 13$ TeV, JHEP 11 (2017) 047. `arXiv:1706.09936, doi:10.1007/JHEP11(2017) 047`.

[36] D. de Florian, et al., Handbook of LHC Higgs Cross Sections: 4. Deciphering the Nature of the Higgs Sector`arXiv:1610.07922, doi: 10.23731/CYRM-2017-002`.

[37] J. Butterworth, et al., PDF4LHC recommendations for LHC Run II, J. Phys. G43 (2016) 023001. `arXiv:1510.03865, doi:10.1088/ 0954-3899/43/2/023001`.

[38] M. Cepeda, et al., Higgs Physics at the HL-LHC and HE-LHC`arXiv: 1902.00134`.

[39] Vector Boson Scattering prospective studies in the ZZ fully leptonic decay channel for the High-Luminosity and High-Energy LHC upgrades, Tech. Rep. CMS-PAS-FTR-18-014, CERN, Geneva (2018).
URL `http://cds.cern.ch/record/2650915`

[40] L. Borgonovi, et al., Higgs measurements at FCC-hh, Tech. Rep. CERN-ACC-2018-0045, CERN, Geneva (Oct 2018).
URL `https://cds.cern.ch/record/2642471`

[41] A. Hocker, et al., TMVA - Toolkit for Multivariate Data Analysis`arXiv: physics/0703039`.

[42] G. Cowan, K. Cranmer, E. Gross, O. Vitells, Asymptotic formulae for likelihood-based tests of new physics, Eur. Phys. J. C 71 (2011) 1554, [Erratum: *Eur. Phys. J. C* **73** (2013) 2501, DOI10.1140/epjc/s10052-013-2501-z]. `arXiv:1007.1727, doi:10. 1140/epjc/s10052-011-1554-0`.